

Visual Analytics Using Heterogeneous Urban Data

Sandro Bonadia*, Rogério Gama*, Daniel de Oliveira*, Fabio Miranda†, Marcos Lage*

*Universidade Federal Fluminense, †University of Illinois Chicago

sbonadia@gmail.com, rogeriogutierrez@id.uff.br, danielcmo@ic.uff.br, fabiom@uic.edu, mlage@ic.uff.br

Abstract—Several cities contain informal settlements in high-risk areas, particularly mountainous regions. With growing concerns around climate change, these areas are more susceptible to environmental disasters, such as floods and landslides, where topography plays a key role. Fortunately, the availability of data describing complex 2D and 3D aspects of urban regions opens new opportunities to tackle these challenges. This paper aims to integrate these data sets to support human-centered solutions. Based on a collaboration with urban planning professionals, we first contribute a data integration framework that takes data from multiple sources with different mathematical descriptions, dimensions, and resolutions and creates a data-enriched triangle mesh that can be used not only for visualization purposes but also in geometry processing and numerical simulation applications. Second, we contribute a visual analytics system that uses the enriched triangulation to enable stakeholders and domain experts to jointly explore a complex and heterogeneous collection of data sets to identify landfall and flood risk areas. Finally, the usefulness of our approach is highlighted through a case study in collaboration with an urban planner interested in risk areas.

I. INTRODUCTION

Throughout history, humans have faced the challenge of where to settle, considering many factors, including climate, availability of resources, *etc.* Today, one can find developed urban centers in multiple areas with different land shapes. For example, Chicago is located in flatlands while Rio de Janeiro is in areas with steep slopes. As these cities grow, the demand for new housing increases, and as land becomes scarce, urban dwellers look to less propitious places to develop, leading to informal settlements. Unplanned urban growth and climate change have led to floods and landslides that killed thousands of people in the past decade around the world [1]. With the urbanization process showing no signs of slowing down and the impacts of climate change becoming more severe, it is increasingly important to understand cities in their full topographical complexity, beyond flatland representations.

The availability of complex data describing multiple aspects of urban areas opens new opportunities for data-driven studies of cities. Problems such as the identification of landslide and flood risk areas can be better studied if we can relate terrain properties (*e.g.*, soil type, height, slope, *etc.*), urban structures (*e.g.*, illegal constructions, paved streets, *etc.*) and spatiotemporal data (*e.g.*, accumulated rain volumes, landslide, and flood occurrences, *etc.*). Depending on the analysis tasks, a visual analytics system designed to tackle urban problems may require not only 2D but also 3D visualizations [2]–[5]. Unfortunately, there is no framework to process and analyze a set of 2D and 3D heterogeneous data (with different mathematical descriptions, dimensions, and resolutions) in an

integrated way. This, in turn, holds back the creation of human-centered solutions that can assist stakeholders in mitigating complex urban problems, such as those caused by unfavorable urban topographies and disordered construction.

Motivated by these challenges and based on the experience acquired over years of collaboration with urban stakeholders, we propose solutions to assist experts in analyzing 2D and 3D heterogeneous data. At the core of our contributions is the need to integrate heterogeneous urban data: (1) vector data describing built environments (*e.g.*, buildings, roads, and parks), (2) raster data (*e.g.*, topography and soil type), and (3) spatiotemporal data sets (*e.g.*, history of rain volumes and landslide incidents). Such integration presents many challenges. First, these heterogeneous data sets come from various sources and are described using different mathematical models, dimensions, and resolutions. Second, data sources have different quality, missing data, and inconsistencies.

Our work then proposes a framework to transform and integrate geographical and spatiotemporal urban data sets containing 2D and 3D information. The framework produces a data-enriched triangle mesh that opens several opportunities for analysis, for example, the computation of new metrics using geometry processing strategies and the simulation of natural phenomena using numerical algorithms. We developed a visual analytics system using the integrated data and conducted case studies to identify landfall and flood risk areas. Our contributions are:

C1. A data framework for integrating different sources, mathematical representations, and spatiotemporal resolutions, including 2D and 3D information. The framework produces a data-rich triangle mesh that can be used for visualization, geometry processing, and numerical simulation proposes.

C2. A visual analytics system, called RISKVIS, to assist experts in identifying landslide and flood risk areas. The system relies on a data-rich triangle mesh integrating terrain, accumulated rain, and historical disaster information.

C3. A case study led by an urban planner from a city in Brazil shows the contribution of the integration framework and visual analytics system to detect landslide and flood risk areas.

Although our research was initially motivated by the need to identify landslide and flood risk regions, the proposed data integration framework and the visual metaphors and interactions used to build RISKVIS can be applied to other problems that benefit from integrating 2D and 3D heterogeneous data.

II. RELATED WORK

Urban Data Integration. Urban data are provided by several sources (ranging from crowdsourced initiatives to the government) using multiple mathematical descriptions, data formats, dimensions, spatiotemporal resolutions, *etc.* Integrating collections of urban data sets is a critical task since it can enable the investigation of real-world problems/phenomena that are hard to observe or reproduce in the real world. Integrated urban data may become rich descriptions of urban areas, especially if inherently 3D data sets and problems are the research targets [6], [7]. Wilson *et al.* [8] discussed different data acquisition strategies and preprocessing methods. The study presents a way of extracting primary terrain parameters (curvature, elevation, *etc.*) that can be obtained from the terrain height data. Bruneton *et al.* [9] presented a method for building detailed renderings of geographical features such as roads, rivers, lakes, *etc.* It uses vector descriptions of geographic features associated with a raster terrain representation. Finally, Over *et al.* [10] presented a solution for generating a 3D map viewer for the web using Open Street Map (OSM) data. The paper describes a data integration process that produces a 3D terrain description based on NASA's SRTM (Shuttle Radar Topography Mission) data and allows the integration of complementary characteristics. Although our paper shares similarities with previous works, it generalizes the data integration process proposed by Over *et al.* [10] to allow the integration of vector, raster, and spatiotemporal data sets from different sources and in various dimensions and resolutions. Also, our approach allows for the generation of independent mesh layers with aligned triangulations. This strategy can help avoid the manipulation of large meshes. For example, one may want to perform a numerical simulation of terrain erosion considering regions identified by the Civil Defense Department as landslide-risk areas and visualize the simulation result as a layer over a 3D map that integrates other aspects of the city as areas containing informal constructions.

Urban Data Analytics. Urban areas are a major source of data with tremendous potential to improve policy-making and the lives of citizens. Visualization systems have long been important for analyzing urban data [7], [11]. Most of these applications use a flat city metaphor to represent the city environment [11]–[15]. On the other hand, cities possess geometric features that are inherently 3D, such as buildings. For this reason, to fully study some problems related to the urban planning and architecture domains, it is crucial to use 3D metaphors for visualizing the city and its associated urban data sets [2], [3], [16]–[19]. Miranda *et al.* [5] proposed a technique to compute accumulated shadow values that enables interactive exploration of what are the shadow patterns over a city during a user-defined period. Although shadow casting is an inherently 3D phenomenon, the work doesn't consider terrain information, making its application restricted to flat cities. Waser *et al.* [20] proposed an interactive 3D visualization to convey how a flooding response plan has to be executed. Although the paper uses fully 3D visualizations, it does not

allow for the integrated visual exploration of multiple data sets. Cornel *et al.* [21] also used proper 3D visualizations to study flood-related hazards, but it focuses on a specific building. Although our work is related to previous works, to the best of our knowledge, this paper proposes the first fully 3D visual analytics framework designed for the interactive and integrated exploration of heterogeneous data sets to support experts and stakeholders in analyzing complex problems such as flood and landslide-risk areas identification.

III. DATA FORMATS AND SOURCES

Some projects (*e.g.*, OSM [22]) and governmental agencies (*e.g.*, NASA [23]) provide 2D geographic data and terrain height information. However, one of the challenges of combining the information in these data sets is that they are described using different strategies: 2D geographical features provided by OSM are described using vector format. In contrast, terrain height information provided by NASA is given in a raster format. If spatiotemporal information, such as rainfall volumes, must be integrated, the problem becomes even more complex. To illustrate the main characteristics of each of these representations, we discuss aspects of vector, raster, and spatiotemporal data sets in the following sections.

A. Vector Data (*e.g.*, OpenStreetMap)

Vector data describes geographic elements as a collection of features (points, lines, and polygons) and attributes. It may represent geographical borders, building footprints, streets, points of interest (POI), *etc.*

One of the most popular vector data sources is the OSM [22] project. Its freely available data is collaboratively curated by the community and contains information on (i) natural elements (vegetation, rivers, *etc.*), (ii) territorial limits (countries, states, *etc.*), and (iii) constructions (buildings, roads, *etc.*) The features provided by OSM are associated with tags that specify their characteristics. Features are described using three data structures (nodes, ways, and relations).

Tags associate attributes to each geographic feature. A tag is a key-value pair, such that the key stores the name of the attribute (*e.g.*, natural, land use), and the value contains the attribute's value (*e.g.*, natural: water, land use: park). *Nodes* are latitude and longitude locations with a unique identification key. A node can represent a point of interest, such as a store, or be part of more complex structures. *Ways* are collections of nodes stored in an ordered list. It describes complex structures such as polylines and polygons used to represent roads, parks, *etc.* The order of the nodes in the list defines the orientation of the way. Similar to the nodes, ways have a unique identification key. Finally, *Relations* are a composition of nodes, ways, or other relations.

Limitations. Although OSM vector data have been used in numerous works [12], [14], the absence of altitude information limits research related to shadows casting [5], view impacts [12], and other inherently 3D problems. Also, since many project contributors are not GIS experts, it is frequent to find inaccurate, incomplete, or inconsistent [24], [25] data.

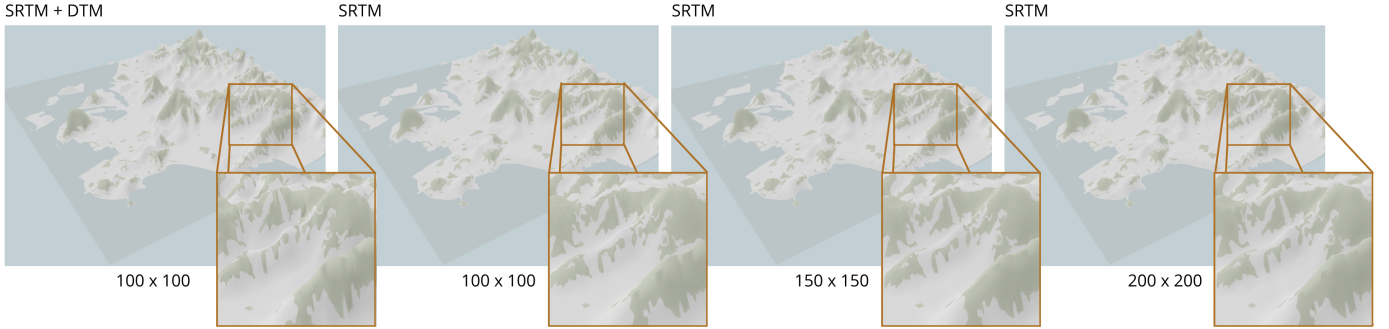


Fig. 1. Integration of OSM vector data and different terrain height raster data. From left to right: the first image shows a terrain produced using the SRTM and DTM data sets. The next three images show terrains generated using only the SRTM data using increasing mesh resolutions.

B. Raster Data (e.g., Terrain Height)

Raster data represents regions as regular grids. The grid cells hold data values, such as rainfall volumes or elevation.

In partnership with the National Imagery and Mapping Agency, NASA produces the SRTM data: a popular terrain height data distributed in raster format for almost the entire planet (with limited resolution). *Digital Terrain Model (DTM)* is another popular topographic model obtained using sensors (such as GPS or LIDAR radars), drones, and even planes. It usually covers smaller areas but provides high-resolution data. It is important to notice that terrain data can have holes caused by failures in their acquisition process. However, as illustrated in Figure 1, when both SRTM and DTM data are available, they can be composed to create high-resolution terrain descriptions of large areas.

C. Spatiotemporal Data (e.g., Rainfall Volume)

Spatiotemporal data contains both space and time-varying information. The spatial component is usually represented as a vector feature or a raster cell, associated with attributes that vary over time. Many open data portals are available [26], some of them maintained by the cities [27]. These portals contain several spatiotemporal data sets. For example, in Brazil, pluviometers are installed nationwide. Data containing the pluviometers' location and their accumulated rain volume measured over time are freely available [28].

IV. DATA INTEGRATION

We propose a data integration framework to combine the raster and vector data, illustrated in Figure 2. The process begins by creating a mesh that covers the entire data set area (see Section IV-A). This mesh serves as a support for the integration process. Then, the raster data sets are associated with each triangle of the mesh (Section IV-B). After, the features of the vector data are localized on the mesh and used to classify and clip vertices and triangles (Section IV-C). Yet, we compose the final meshes that integrate the raster information on their vertices and approximate the geometry of vector data (Section IV-D). It is worth stressing that the process is not dependent on any specific data set. Also, the framework produces independent and aligned triangle meshes for each input collection of vector features.

A. Base Mesh Construction

The base mesh is the reference for the construction of all map layers. To build the mesh, we first construct a regular grid spanning the data set coverage area based on a user-defined resolution. Once the grid is created, each cell is subdivided into two triangles. We notice that the resolution of the base mesh is directly related to the produced result. Figure 1 shows meshes made using SRTM and OSM data. The resolution of the base meshes varies from 100×100 to 200×200 grid cells. As one can see, more detailed relief meshes are produced as the resolution increases.

We use a topological data structure to store the triangulation, a simplified version of the CHE (Compact Half-Edge) [29]. The data structure allows for fast topological queries even for large meshes. Efficiently traversing the mesh and extracting information such as adjacent triangles and vertices are capabilities required by the raster smoothing (Section IV-B) and the mesh classification and clipping (Section IV-C) operations. We also use the data structure to store the vertices' coordinates, normal vectors, and information smoothed from raster data or derived from the mesh (e.g., slope).

B. Raster Data Smoothing

We start by associating each raster cell with its overlapping base mesh triangles. After this operation, some triangles may have no associated data, depending on the raster data and base mesh resolutions. To avoid the occurrence of these artificial holes, we compute the median of the raster data stored in the neighborhood (orange triangles on Figure 2 (b)) of each triangle. Once all triangles are associated with a median value, we extrapolate this information to each vertex of the mesh by averaging the values of the triangles inside a smoothing circle centered on the vertex (orange circle in Figure 2 (b)). We observe that data sets holding complementary information can be merged in this step. For example, SRTM and DTM can be used to create more detailed terrain meshes (Figure 1 (a-b)).

C. Base Mesh Classification and Clipping

After associating the raster data with the vertices of the base mesh, we classify the mesh triangles considering the features of the input vector data. Given the base mesh and a

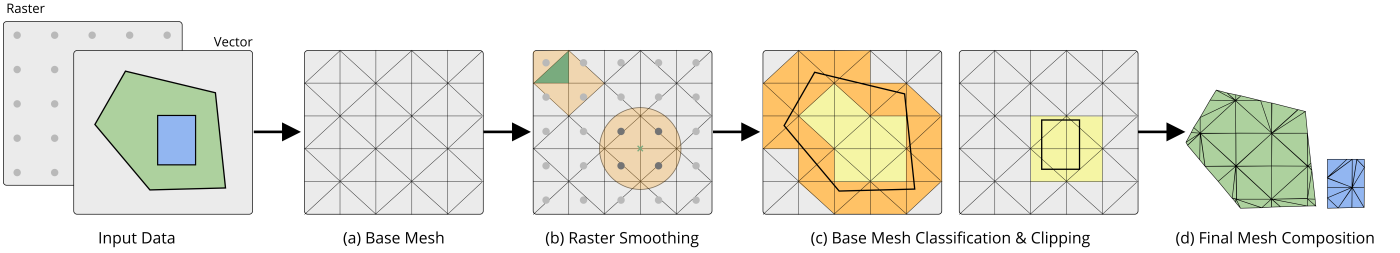


Fig. 2. Vector and Raster data integration. (a) We build a triangle mesh covering the input data domains. (b) Raster data are associated with the vertices of the mesh. (c) Vector data are used as clipping masks. (d) The clipped triangles compose a mesh combining the vector data geometry and the raster information.

set of vector features, we iterate over each feature to identify triangles completely inside, partially contained, and outside the features (yellow, orange, and gray triangles in Figure 2 (c), respectively). Triangles that fall entirely inside the features are trivially classified as part of the final mesh. Similarly, triangles that are totally outside the features are discarded. Finally, triangles partially inside the features are clipped and re-meshed. We used the Weiler–Atherton [30] and the Ear Clipping [31] algorithms to perform these operations. Finally, we approximate the raster data in each point generated during clipping using the approach described in the previous section.

D. Final Mesh Composition

The triangles produced by the clipping step are combined with the base mesh ones considered inside the features to compose the final mesh (see Figure 2 (d)). The produced triangulation approximates the geometry of the vector features and holds raster data from the input. Moreover, it is possible to enrich the mesh by joining spatiotemporal urban data information, computing geometric attributes such as curvatures and slope angle (or any other property added using a mesh-based algorithm), simulating numerical equations, and storing the additional data in the vertices of the final mesh.

V. VISUAL ANALYSIS OF RISK AREAS

Motivated by the possibilities that emerge from the data integration framework, we developed a visual analytics system called RISKVIS, designed to help stakeholders identify landslide and flood risk areas. It enables the visual exploration of a data-rich 3D mesh representation of a mountainous city in Brazil built using OSM features, raster terrain data, and rainfall-related spatiotemporal urban data sets.

A. Data Description and Management

We use DTM data captured in 2014 in the studied city. Although this data set contains high-resolution relief information, it does not cover some parts of the city. For this reason, we combined it with NASA's SRTM data to represent the entire city's terrain. We also used data from the city administration delimiting known risk areas and *favelas*. Finally, we integrated the history of rainfall volumes, landslides, and flood occurrences between years 2010 and 2021.

To accelerate queries to the information stored in the vertices of the data-rich mesh produced by the integration

framework, the vertex data were ingested into a MonetDB database [32]. MonetDB is an open-source database management system (DBMS) focused on OLAP (Online Analytical Processing) and Big Data queries, which can load bulk data quickly by benefiting from multiple cores and CPUs. The database schema used by RISKVIS contains two tables: (i) the *Mesh Data* and (ii) *Event Occurrence*. The data stored on the mesh's vertices are loaded into the Mesh Data table. The data associated with the events (date and time, reason, type, and location) are loaded into the Event Occurrence table. We can efficiently discover events close to mesh vertices and *vice-versa* using these tables.

B. Visual Interface

The visual interface of RISKVIS comprises three linked visualization widgets, shown in Figure 3: the 3D Map, the Mesh Projection, and the Rain & Occurrences Matrix.

3D Map. The 3D Map widget visualizes the data-rich 3D mesh produced by the integration framework. It is essential to use a 3D visualization since the goal of RISKVIS is to identify risk areas, which are heavily determined by their 3D structure.

Mesh Projection. The Mesh Projection widget was developed to allow users to identify mesh vertices storing similar values. The widget contains two rings and a central projection area. The external ring's sectors represent the terrain's characteristics (*e.g.*, landuse, and slope) and are colored using a categorical color scale. Each sector of the internal ring is associated with one of the external sectors and represents a possible value of the related characteristic. The colors of the inner sectors range from light to dark shades of gray and illustrate the number of vertices of the terrain associated with the value. The sectors of both rings can be clicked to filter and highlight points in the central projection and on the map. The center area shows the t-SNE [33] projection of the mesh vertices and their associated attributes. Projected vertices can be brushed to update the distribution of attributes represented by the internal and external rings. They are highlighted on the map, facilitating the localization of similar regions.

Rain & Occurrences Matrix. The Rain & Occurrences Matrix has a vertical axis representing a discrete scale of accumulated rain values (no rainfall, light rainfall, medium rainfall, heavy rainfall, torrential rainfall), and the horizontal axis represents a time interval (ranging from 15 minutes to 24 hours). The color of each square represents the number

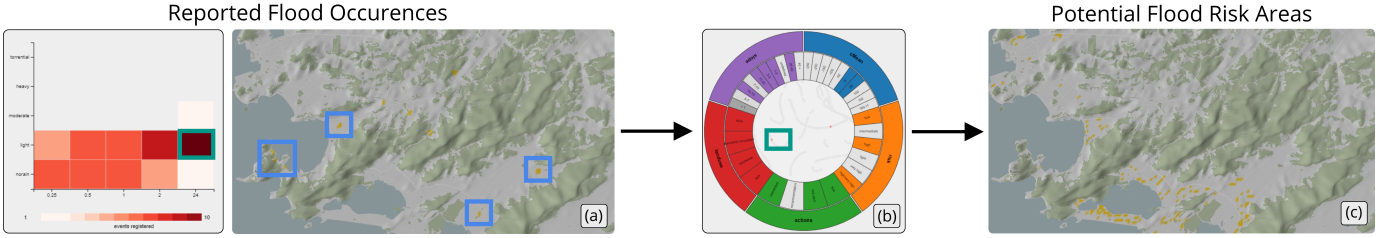


Fig. 3. (a) The heat matrix shows flood occurrences (colors from white to red) for different measurement periods and rain intensity pairs. The green rectangle selects the persistent-light rain scenario, and the associated areas are highlighted in yellow on the map. Since the number of flood reports is usually small (blue rectangles), many well-known flood areas are not displayed on the map. (b) Using the Mesh Projection widget, the expert could identify regions similar to the occurrences areas. (c) The Figure shows, highlighted in yellow, areas with potential flood risk.

of occurrences reported when an accumulated rain value is observed during a time interval. The heat matrix squares are clickable. Mesh vertices close to the events associated with the square are highlighted in the Mesh Projection widget and on the 3D map. The Heat Matrix Widget also enables filtering occurrences by type (landslide or flood).

VI. CASE STUDIES: IDENTIFICATION OF RISK AREAS

To validate RISKVIS, we interviewed an urban planning specialist, co-author of the paper. We introduced him to the system, and then he independently used the system in a recorded session. His findings are described next.

Flood Risk Areas. The studied city has an ancient drainage infrastructure that has grown in a poorly planned way over the years. The expert observed that mapping flood risk areas is difficult since most flood occurrences do not cause severe damage or death. So, the number of reported events is small and does not include all problematic city locations. The expert started using the Rain & Occurrences Matrix to filter flood-risk regions based on the occurrences reported in the past. The green box over the widget in Figure 3(a) shows that he used the heat matrix to select rain scenarios with more reported occurrences. The regions on the map inside the blue squares show where these flood occurrences happened. Using the Mesh Projection widget, the expert selected a cluster of points close to the projection of occurrence locations. These areas have characteristics similar to the regions where floods were reported (see the green rectangle in Figure 3(b)). As shown in Figure 3(c), many other city areas are highlighted. It is known that some of these regions suffer from floods, although no occurrences were reported at these locations. The expert observed that these regions should also be considered in future drainage actions.

Landslide Risk Areas. The expert enjoyed visually exploring data of different natures, such as terrain slope, land use, and rainfall volume. He observed that connections among these attributes are vital for decision-making on public policies, civil defense prevention strategies, or even urbanization projects. Initially, he used the Mesh Projection widget to highlight risk areas identified by the Civil Defense Department (see Figure 4(a)). As the image shows, just a few places are highlighted on the map. Next, he used the Mesh Projection to select mesh vertices with *favela* classification and a slope

greater than 15°. Doing so, he could observe areas of the city that potentially have a high occurrence risk (see Figure 4(b)). To better understand the coverage of the Civil Defense risk classification, areas classified by the department as high-risk areas were filtered using the same criteria (*favela* land use and a slope greater than 15°). As shown in Figure 4(c)), the number of spotlighted regions is small. Using the system, the specialist could observe that areas tagged as high risk by the authorities are restricted to a small portion of the city. Also, he commented that the 3D visualization shows that some risk areas may impact important surrounding regions (e.g., streets and roads), which may be considered in decision-making. In conclusion, he observed that the system helped identify regions with potentially dangerous characteristics not recognized as risk areas by public administration.

As final feedback, the specialist observed that the tool could be handy for building high-precision risk area reports since geological mappings are usually done using separate terrain data loaded on off-the-shelf software that frequently limits the identification of micro-scale risk regions.

VII. CONCLUSION

Open urban data are made available from different sources in several formats, resolutions, and mathematical descriptions, increasing the difficulty to use them. The data integration framework proposed in this paper aims to facilitate access to such data. In particular, we showed how vector, raster, and spatiotemporal data can be combined to create data-rich meshes describing cities. Moreover, the visual analysis of these meshes can impact decision-making and help public agents to propose better urbanization policies. The RISKVIS system illustrates that important actions (such as identifying landslide and flood risk areas) can be more effective when guided by integrated data analysis. In future work, we plan to use the integration framework to create detailed descriptions and visual analytics applications to study *favelas*. Another future work direction is integrating data sets related to sidewalk networks and computing accessibility metrics, such as sidewalk slopes.

REFERENCES

- [1] A. Busch and S. Amorim, “A tragédia da região serrana do Rio de Janeiro em 2011: Procurando respostas,” Escola Nacional de Administração Pública (ENAP), Tech. Rep. 2, 2011.

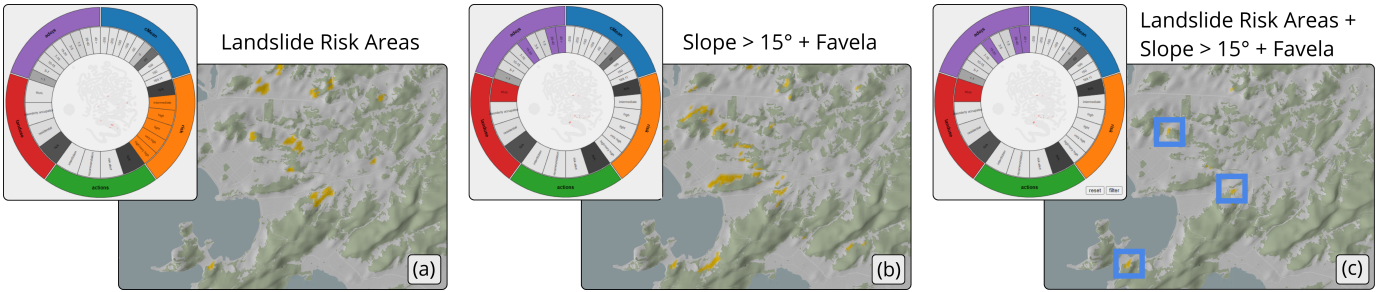


Fig. 4. (a) The Mesh Projection visualization was used to filter areas identified by the Civil Defense Department as risk areas, also highlighted in yellow on the map. (b) Filtering *favela* areas with terrain slope greater than 15° , we observe (highlighted in yellow on the map) many areas with informal constructions in high-slope terrains. These characteristics, when observed together, increase the chances of landslides. (c) The figure shows that just a few *favela* locations (blue rectangles) having a terrain slope greater than 15° are already identified as risk areas by the public administration.

- [2] N. Ferreira, M. Lage, H. Doraiswamy, H. Vo, L. Wilson, H. Werner, M. Park, and C. Silva, "Urbane: A 3D framework to support data driven decision making in urban development," in *2015 IEEE Conference on Visual Analytics Science and Technology (VAST)*, 2015, pp. 97–104.
- [3] H. Doraiswamy, N. Ferreira, M. Lage, H. Vo, L. Wilson, H. Werner, M. Park, and C. Silva, "Topology-based catalogue exploration framework for identifying view-enhanced tower designs," *ACM Transactions on Graphics (TOG)*, vol. 34, no. 6, pp. 1–13, 2015.
- [4] H. Doraiswamy, E. Tzirita Zacharatuou, F. Miranda, M. Lage, A. Ailamaki, C. T. Silva, and J. Freire, "Interactive visual exploration of spatio-temporal urban data sets using urbane," in *Proceedings of the 2018 International Conference on Management of Data*, ser. SIGMOD '18. ACM, 2018, pp. 1693–1696.
- [5] F. Miranda, H. Doraiswamy, M. Lage, L. Wilson, M. Hsieh, and C. T. Silva, "Shadow accrual maps: Efficient accumulation of city-scale shadows over time," *IEEE Transactions on Visualization and Computer Graphics*, vol. 25, no. 3, pp. 1559–1574, 2018.
- [6] F. Biljecki, J. Stoter, H. Ledoux, S. Zlatanova, and A. Çöltekin, "Applications of 3D city models: State of the art review," *ISPRS International Journal of Geo-Information*, vol. 4, no. 4, pp. 2842–2889, 2015.
- [7] H. Doraiswamy, J. Freire, M. Lage, F. Miranda, and C. Silva, "Spatiotemporal urban data analysis: A visual analytics perspective," *IEEE Computer Graphics and Applications*, vol. 38, no. 5, pp. 26–35, 2018.
- [8] J. P. Wilson, "Digital terrain modeling," *Geomorphology*, vol. 137, no. 1, pp. 107–121, 2012.
- [9] E. Bruneton and F. Neyret, "Real-time rendering and editing of vector-based terrains," *Computer Graphics Forum*, vol. 27, 2008.
- [10] M. Over, A. Schilling, S. Neubauer, and A. Zipf, "Generating web-based 3D city models from OpenStreetMap: The current situation in Germany," *Computers, Environment and Urban Systems*, vol. 34, no. 6, p. GeoVisualization and the Digital City, 2010.
- [11] Y. Zheng, W. Wu, Y. Chen, H. Qu, and L. M. Ni, "Visual analytics in urban computing: An overview," *IEEE Transactions on Big Data*, vol. 2, no. 3, pp. 276–296, 2016.
- [12] N. Ferreira, J. Poco, H. T. Vo, J. Freire, and C. T. Silva, "Visual exploration of big spatio-temporal urban data: A study of new york city taxi trips," *IEEE Transactions on Visualization and Computer Graphics*, vol. 19, no. 12, pp. 2149–2158, 2013.
- [13] J. Zhang, E. Yanli, J. Ma, Y. Zhao, B. Xu, L. Sun, J. Chen, and X. Yuan, "Visual analysis of public utility service problems in a metropolis," *IEEE Transactions on Visualization and Computer Graphics*, vol. 20, no. 12, pp. 1843–1852, 2014.
- [14] F. Miranda, H. Doraiswamy, M. Lage, K. Zhao, B. Gonçalves, L. Wilson, M. Hsieh, and C. T. Silva, "Urban Pulse: Capturing the rhythm of cities," *IEEE Transactions on Visualization and Computer Graphics*, vol. 23, no. 1, pp. 791–800, 2016.
- [15] A. Karduni, I. Cho, G. Wessel, W. Ribarsky, E. Sauda, and W. Dou, "Urban space explorer: A visual analytics system for urban planning," *IEEE Computer Graphics and Applications*, vol. 37, no. 5, pp. 50–60, 2017.
- [16] J. Wendel, S. M. Murshed, A. Sriramulu, and A. Nichersu, "Development of a web-browser based interface for 3D data — A case study of a plug-in free approach for visualizing energy modelling results," May 2016, pp. 185–205.
- [17] T. Ortner, J. Sorger, H. Steinlechner, G. Hesina, H. Piringer, and E. Gröller, "Vis-a-wake: Integrating spatial and non-spatial visualization for visibility-aware urban planning," *IEEE Transactions on Visualization and Computer Graphics*, vol. 23, no. 2, pp. 1139–1151, 2016.
- [18] W. Zeng and Y. Ye, "VitalVizor: A visual analytics system for studying urban vitality," *IEEE Computer Graphics and Applications*, vol. 38, no. 5, pp. 38–53, 2018.
- [19] B. Mao, Y. Ban, and B. Laumert, "Dynamic online 3D visualization framework for real-time energy simulation based on 3D tiles," *ISPRS International Journal of Geo-Information*, vol. 9, no. 3, 2020.
- [20] J. Waser, A. Konev, B. Sadransky, Z. Horváth, H. Ribićić, R. Carneky, P. Kluding, and B. Schindler, "Many plans: Multidimensional ensembles for visual decision support in flood management," in *Computer Graphics Forum*, vol. 33, no. 3. Wiley Online Library, 2014, pp. 281–290.
- [21] D. Cornel, A. Konev, B. Sadransky, Z. Horvath, E. Gröller, and J. Waser, "Visualization of object-centered vulnerability to possible flood hazards," in *Computer Graphics Forum*, vol. 34, no. 3. Wiley Online Library, 2015, pp. 331–340.
- [22] OpenStreetMap contributors, "Planet Dump," 2017. [Online]. Available: <https://planet.osm.org>
- [23] T. G. Farr, P. A. Rosen, E. Caro, R. Crippen, R. Duren, S. Hensley, M. Kobrick, M. Paller, E. Rodriguez, L. Roth, and others, "The shuttle radar topography mission," *Reviews of geophysics*, vol. 45, no. 2, 2007.
- [24] S. S. Sehra, J. Singh, and H. S. Rai, "A Systematic Study of OpenStreetMap Data Quality Assessment," in *2014 11th International Conference on Information Technology: New Generations*, 2014, pp. 377–381.
- [25] P. Mooney, P. Corcoran, and A. C. Winstanley, "Towards quality metrics for OpenStreetMap," in *Proceedings of the 18th SIGSPATIAL international conference on advances in geographic information systems*, 2010, pp. 514–517.
- [26] M. L. A. Díez, "Linked open data portals: functionalities and user experience in semantic catalogues," *Online Inf. Rev.*, vol. 45, no. 5, pp. 946–963, 2021.
- [27] "NYC Open Data," Jul. 2022. [Online]. Available: <https://nycopendata.socrata.com/>
- [28] "Sistema De Gestão de Geoinformação," Jul. 2022. [Online]. Available: <https://www.sigeo.niteroi.rj.gov.br/>
- [29] M. Lage, T. Lewiner, H. Lopes, and L. Velho, "CHE: A scalable topological data structure for triangular meshes," *Department of Mathematics, Pontifícia Universidade Católica—Rio de Janeiro, Brazil*, 2005.
- [30] G. Greiner and K. Hormann, "Efficient clipping of arbitrary polygons," *ACM Transactions on Graphics (TOG)*, vol. 17, no. 2, pp. 71–83, 1998.
- [31] D. Eberly, "Triangulation by ear clipping," *Geometric Tools*, pp. 2002–2005, 2008.
- [32] S. Idreos, F. Groffen, N. Nes, S. Manegold, K. S. Mullender, and M. L. Kersten, "Monetdb: Two decades of research in column-oriented database architectures," *IEEE Data Eng. Bull.*, vol. 35, no. 1, pp. 40–45, 2012.
- [33] L. Van der Maaten and G. Hinton, "Visualizing data using t-SNE," *Journal of machine learning research*, vol. 9, no. 11, 2008.